Journal Pre-proof

Electrochemically Assisted Photocatalysis for the Disinfection of Rainwater under Solar Irradiation

S. McMichael (Conceptualization) (Investigation)<ce:contributor-role>Writing-original draft)<ce:contributor-role>Writing-review and editing), M. Waso (Methodology)<ce:contributor-role>Writing-review and editing), B. Reyneke (Methodology)<ce:contributor-role>Writing-review and editing), W. Khan (Funding acquisition) (Supervision) (Methodology)<ce:contributor-role>Writing-review and editing), J.A. Byrne (Funding acquisition) (Supervision)<ce:contributor-role>Writing-review and editing), P. Fernandez-Ibanez (Funding acquisition) (Supervision)<ce:contributor-role>Writing-review and editing)

PII: S0926-3373(20)30900-0

DOI: https://doi.org/10.1016/j.apcatb.2020.119485

Reference: APCATB 119485

To appear in: *Applied Catalysis B: Environmental*

Received Date: 24 June 2020

Revised Date: 20 August 2020

Accepted Date: 24 August 2020

Please cite this article as: McMichael S, Waso M, Reyneke B, Khan W, Byrne JA, Fernandez-Ibanez P, Electrochemically Assisted Photocatalysis for the Disinfection of Rainwater under Solar Irradiation, *Applied Catalysis B: Environmental* (2020), doi: https://doi.org/10.1016/j.apcatb.2020.119485

Electrochemically Assisted Photocatalysis for the Disinfection of Rainwater under Solar Irradiation

S. McMichael[1]*, M. Waso[2], B. Reyneke[2], W. Khan[2], J.A. Byrne[1], P. Fernandez-Ibanez*[1]

[1]NIBEC, Ulster University, Newtownabbey, BT37 0QB, United Kingdom

[2] Department of Microbiology, Stellenbosch University, Stellenbosch, 7602, South Africa

*Corresponding authors: mcmichael-s@ulster.ac.uk

p.fernandez@ulster.ac.uk

Graphical abstract

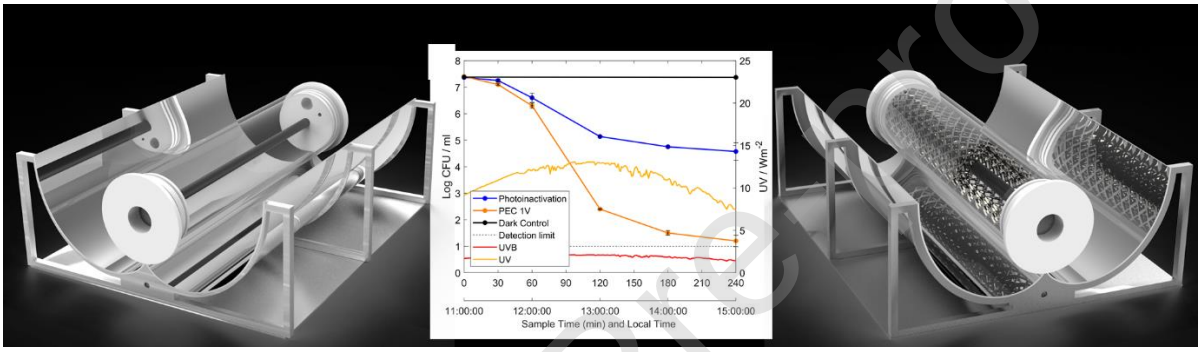

Highlights

- Photoelectrocatalytic (PEC) reactor tested under natural sunlight during winter.
- Environmental strains of Escherichia coli and Pseudomonas aeruginosa inactivated.
- Viability of bacteria assessed by culture and molecular (EMA-qPCR) methods.
- PEC showed 2.2±3.8 higher inactivation rates than solar disinfection.

Abstract

In this work a photo electrochemical reactor (PEC) with a compound parabolic collector (CPC) has been designed and tested for the electrochemically assisted photocatalytic (EAP) disinfection of rainwater under real sun conditions in South Africa. The reactor consisted of a Ti mesh coated with aligned titania nanotubes with a carbon counter electrode in a concentric tubular configuration, within a borosilicate glass tube with a CPC. Environmental strains of *Escherichia coli* and *Pseudomonas aeruginosa* were used. The viability of the microorganisms

was analysed by culture-based and by EMA-qPCR methods. The reactor was tested under real sun during the winter in South Africa with a relatively low UV irradiance (max: 13 Wm-2). Under real sun irradiation, EAP yielded a 6.2-log10 reduction for *E. coli* and a 5.4-log10 reduction for *P. aeruginosa* for culture-based analysis. The EAP treatment also showed improved results by EMA-qPCR analysis with a 2.4-log10 reduction in gene copies for *E. coli* and 3.0-log10 for *P. aeruginosa.*

Keywords: TiO_2 Nanotubes, Solar Disinfection, EMA-qPCR, Electrochemically Assisted Photocatalysis, *Pseudomonas aeruginosa*

1. Introduction

The world faces many water related challenges, with 2 billion people lacking access to a safe source of drinking water, 2.55 billion people affected by water shortages and 1.9 billion people affected by water scarcity [1, 2]. To combat the problem of fresh water shortages and scarcity, domestic rainwater harvesting and storage has been implemented in many countries, for example: Nigeria, South Africa, Australia and the USA [3].

The potential use of rainwater varies between countries, from irrigation and vehicle washing, to potable water [3]. Nevertheless, the quality of harvested rainwater depends on the atmospheric conditions and the harvesting system employed. The rainwater may be polluted by suspended and dissolved matter from the atmosphere, and harvested rainwater may be polluted by chemical and microbiological contaminants from the collection surface (normally the house roofing), piping and storage system. Contamination from roofing materials can result in dissolved metal concentrations exceeding the World Health Organisation (WHO) drinking water guidelines e.g. the OLPLWRIJ/ $^{-1}$ of lead is commonly exceeded [4]. Microbial and parasite contamination due to animal faeces is of major concern and is influenced by seasonal and environmental conditions. Bacterial pathogens commonly found in harvested rainwater include, *Campylobacter* spp., *Salmonella* spp., *Shigella spp., Vibrio* spp., and other opportunistic bacterial and parasitic pathogens such as *Aeromonas spp., Pseudomonas* spp., *Legionella* spp., *Mycobacterium* spp., *Cryptosporidium* spp., and *Giardia* spp. [4, 5]. If the harvested rainwater is to be used for irrigation of food crops or as potable water, pathogenic microorganisms must be removed or inactivated. Any technology used for disinfection for

potable water should achieve the standards indicated by the WHO drinking water guidelines [6]. For applications in the Development Assistance Committee list of low-to-middle-income countries the cost of treatment should be kept to a minimum without compromising on the efficacy of disinfection, and ideally should provide sufficient, acceptable and accessible potable water.

Household water treatment solutions have been evaluated by the WHO and reported in the International Scheme to Evaluate Household Water Treatment Technologies [7]. Appropriate treatment methods include ultrafiltration, chlorination and solar disinfection. However, ultrafiltration is expensive and requires accessible replacement of filters. Chlorination is low cost and effective, however, if the dose is too high it affects palatability and can produce potential carcinogenic by-products such as trihalomethanes [8]. Furthermore, some viruses and protozoa are highly resistant to chlorination and the chlorine dose is difficult to control based on chlorine demand [9]. Of course other disinfection solutions are available but all have their own drawbacks e.g. UVC requires specialized lamps and ozone requires a generator, and it is well known that some microorganisms are resistant to UVC and ozone. While, solar disinfection has been extensively investigated [10-12]; disadvantages include long exposure times and the lack of quality assurance. Additionally, the rate of solar photo-inactivation is dependent on the solar irradiance and some microorganisms are more resilient to solar inactivation, such as *Pseudomonas aeruginosa* [13].

Heterogeneous photocatalysis has been reported to be effective for the inactivation of a wide range of microorganisms (viruses, protozoa and bacteria) and for the degradation of a wide range of chemical compounds found in water [14]. Titanium dioxide (TiO_2) is the most commonly employed photocatalyst for water treatment applications. Upon excitation with UV photons, electron-hole pairs are formed which can either recombine releasing energy, or react with water and oxygen at the interface to generate reactive oxygen species (ROS) (Figure 1, left). In simple photocatalytic systems, the photocatalyst is added to the water as a powder suspension; however, using micro or nanoparticle photocatalysts in suspension-based systems requires post-treatment removal of the catalyst, adding cost and complexity to the system. Although, immobilisation of the photocatalyst onto supporting substrates has been studied [15], this reduces the specific surface area in contact with solution and introduces mass transport limitations to the reaction system. Therefore, immobilised systems tend to be less effective than slurry-based systems [16]. TiO_2 (and other materials) exhibits fast recombination of

photogenerated charge carriers, thus reducing the quantum yield for the production of ROS [17]. In electrochemically assisted photocatalysis (EAP), the photocatalyst is immobilised on an electrically conducting support which acts as a photoanode in a two electrode cell where the application of an external electrical bias assists charge separation and improves the overall efficiency (Figure 1) [18]. EAP has other advantages as compared to photocatalytic systems, where the sites for oxidation and reduction are spatially separated, reducing surface recombination reactions. The photocurrent will be proportional to the irradiance in the band gap region and can be used to control the residence time in the reactor. Electromigration of negatively charged species to the photoanode may also improve mass transport. Of course, photoelectrochemical cells (PEC) are more complex to fabricate and are likely to have a higher capital cost than photocatalytic systems. EAP, like photocatalysis, does not require the addition of consumable chemicals other than oxygen from the air. To improve the solar efficiency, novel materials are required which can utilize visible photons. Other solar driven AOPs are not suitable for the treatment of potable water e.g. photo-Fenton requires the addition of iron and peroxide.

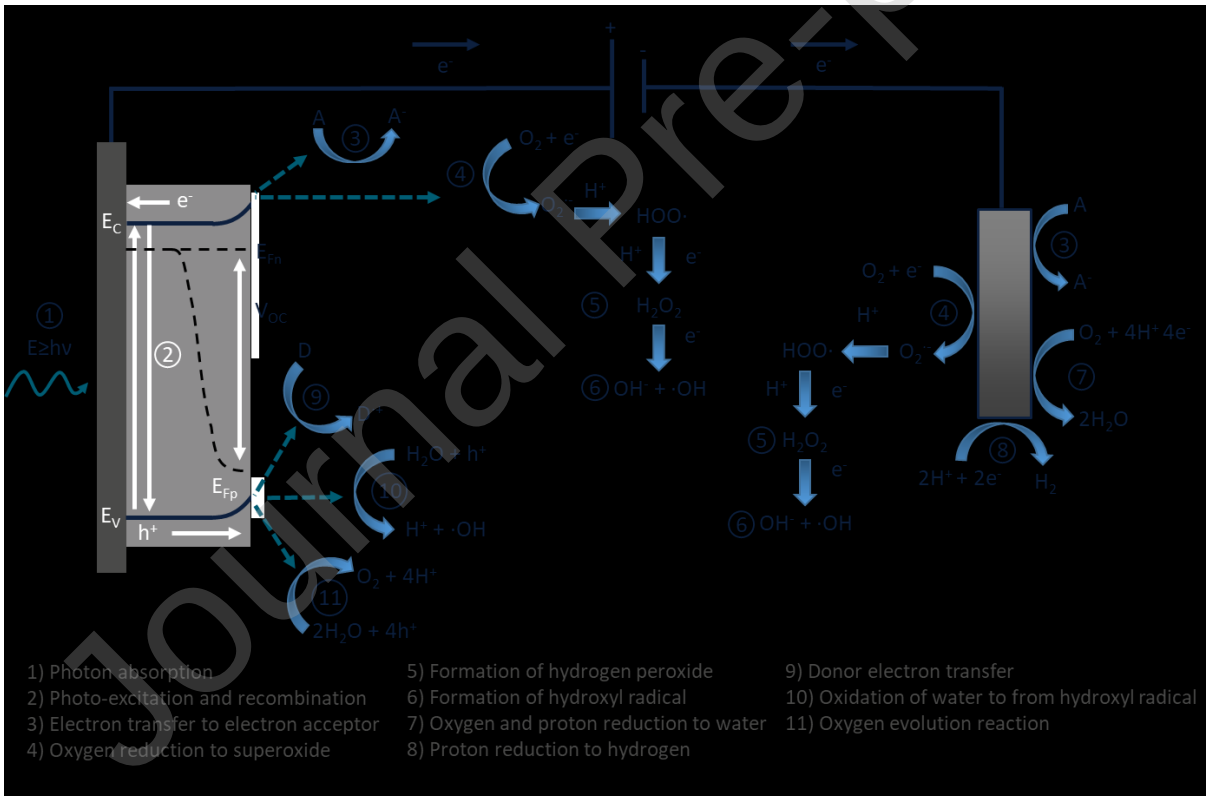

Figure 1 ± Diagram of the EAP process and pathways for radical production using a photoanode and a non-semiconducting counter electrode

Nanoengineering of TiO_2 can be achieved by electrochemical anodisation of Ti metal in the presence of fluoride which results in the formation of aligned self-organised titania nanotubes (TiNT). These electrodes have been reported to have a higher photocurrent density and improved disinfection efficiency, as compared to nanoparticulate or compact oxide electrodes; this is due in part to the short diffusion path for photoinduced holes and a direct path for photoinduced electrons to the supporting electrode [19]. Additionally, the in-situ growth of the oxide on the parent titanium metal improves the adhesion of the titania and increases electrode stability [20].

Carbon felt can be used as a low-cost, flexible counter electrode which can selectively reduce oxygen to hydrogen peroxide [21]. This is a disinfectant product which has a long lifetime in the range of hours to days depending on the environment, enabling long diffusion length from the surface of the electrode into the bulk solution [22, 23].

For the first time we have applied TiNT photoanodes with a carbon cathode in a CPC reactor for the EAP disinfection of rain water under real sun. Two reactors were tested in parallel, one with EAP and one without EAP as a control (photo-inactivation). Two bacterial strains were used as model organisms, *E. coli* and *P. aeruginosa*, and viability was determined by culture based and molecular methods.

2. Materials and methods

2.1 Materials & Chemicals

The materials and chemicals used are as follows: titanium mesh (Titanium Metals UK Ltd), Duran borosilicate glass tube (SCHOTT), reflective aluminum (Alanod GmbH), ethylene glycol (anhydrous 99.8% from Sigma-Aldrich), stainless-steel rod 316 (Aalco), carbon felt (Alfa Aesar), nutrient broth (Millipore), agar (Millipore), NaCl (Millipore), ethidium monoazide (Biotium), *Quick*-16S Microbe Miniprep Kit (Zymo Research), and FastStart Essential DNA Green Master Mix (Roche Applied Science).

2.2 Reactor configuration & Experimental set-up

The PEC reactor as shown in Figure 2 is of cylindrical based geometry; this was to enable the use of a CPC with a concentration factor of 1; which increases the solar irradiation directed into the reactor. The reactor container was a borosilicate tube with an external diameter of 50 mm, capped at the bottom with a custom-made endcap to allow air purging, and had a working volume of 300 ml. The photoanode was titanium mesh (64% open area) coated with self-organised TiNT. The mesh allows for the mass transport between the photoanode and the cathode, as well as allowing a percentage of the solar irradiation to pass through the reactor reducing unilluminated areas; as dark areas enable bacteria to undergo a dark-activated repair mechanism [24]. The high open area of the mesh reduces the surface area for photon DEVRUSWLRQ WKHUHIRUH WZR F\OLQGULFDO PHVK¶V ZKHUH XVHG HDFK ZLWK D GLIIHUH placed inside one another as shown in the cross sectional view in Figure 2. The calculated open area of the two meshes is 17%. The cathode consisted of a 3 mm diameter stainless-steel rod wrapped with carbon felt. The cylindrical design results in the placement of the cathode at the center of the reactor. This may cause dark areas to be formed within the reactor, but it is mitigated by using the CPC which acts as a non-imaging concentrator that reflects the diffuse solar UV regardless of the angle and the time of the day, leading to a concentration factor of 1, so that the reactor tube is illuminated by one-sun equivalent in the UV range all the time [25]. The CPC mirror is made of anodised aluminum to maximise the reflectance of UV, as reported elsewhere [26, 27].

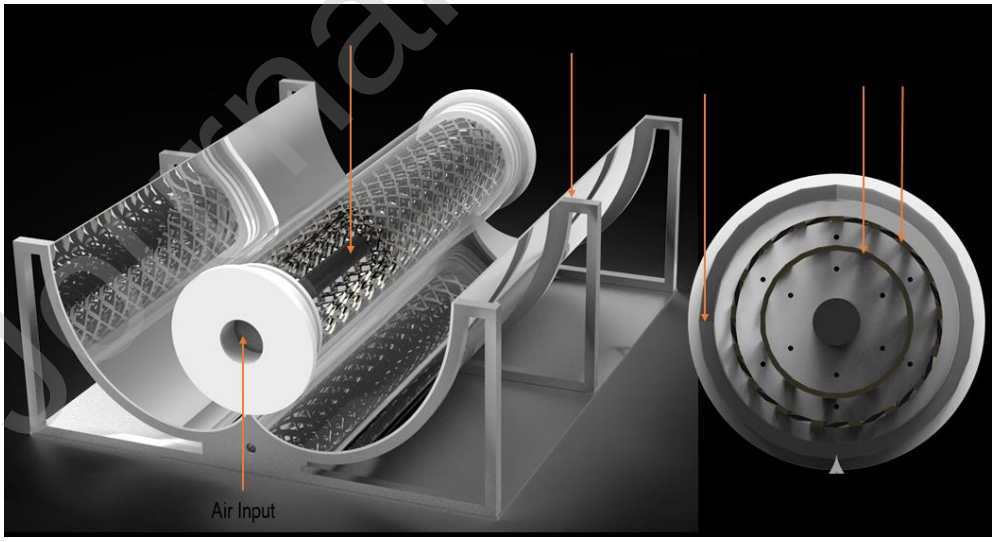

Figure 2- PEC reactor configuration

To assess the effect of only solar disinfection (photo-inactivation) a second reactor was tested in tandem. This reactor was of the same geometry, with a CPC but contained only the carbon felt on a stainless steel rod as this may act as a solar thermal heater. Solar disinfection may be enhanced by thermal effects but these only become important above 40ºC [14].

The solar CPC-PEC reactors were tested using rainwater harvested from a local community site (Bonfoi, Stellenbosch, South Africa). The pH, electrical conductivity and total dissolved solids present in harvested rain water before and after autoclaving using a hand-held Milwaukee Instruments MI806 meter (Spraytech, South Africa), and the dissolved oxygen using a Milwaukee Instruments M600 meter (Spraytech, South Africa). These parameters were not markedly affected by autoclaving and remained within the general range reported for the Bonfoi site (Stellenbosch, South Africa) (Table 1). The conductivity of the rainwater sample used for the disinfection experiments was 70 µScm^{-1} at 21ºC. The rainwater was then spiked with the model organisms, i.e. *Escherichia coli* (*E. coli*) and *Pseudomonas aeruginosa* (*P. aeruginosa*) strains isolated from rainwater samples (section 2.5ZLWKDFRQFHQWUDWLRQ• log CFU ml^{-1}.

The disinfection experiments where conducted in duplicate for each organism. The time taken for experiments meant that repeat runs had to be conducted on consecutive days. The solar UV irradiance during these experiments was similar. For the *E. coli* experiments, the average UV (280-400 nm) irradiance on the two days was 10.8 W m^{-2} and 11.2 W m^{-2}, (3.6% difference) with a maximum irradiance of 16.1 W m^{-2} and 11.2 W m^{-2}. For *P. aeruginosa* experiments the average UV irradiance on the two days was 13.3 W m^{-2} and 10.7 W m^{-2} (19.5% difference) with a maximum irradiance of 11.3 W m^{-2} and 12.4 W m^{-2}.

A cell bias of 1.0 V was used based on the *I-V* curve (Figure 5) of the PEC system (TiNT - mesh as the anode). The CPC-PEC reactor was angled at approximately 51º which is just slightly lower than the optimal angle for the specific day (~57º, coordinates 33.93º S, 18.86º E) to have the maximum solar irradiation at solar noon [28].

The UV data for the days in which the experiments where conducted was obtained from Stellenbosch Weather Services, Engineering Faculty, Stellenbosch University: http://weather.sun.ac.za. A Kipp & Zonen UVS-AB-T radiometer with solar tracking was used to measure the power density (Wm^{-2}) for UVA between 315 - 400 nm and UVB between 280 - 315 nm at 1 min intervals.

Table 1 - Mean physico-chemical parameters recorded in untreated rainwater and after the rainwater was sterilised by autoclaving.

Parameter	Untreated Rainwater	Autoclaved Rainwater	Range reported for rainwater collected from the Bonfoi community site [29]
pH	7.40 ± 0.01	8.60 ± 0.08	5.66 ± 8.85
Dissolved oxygen (mg L^{-1})	5.30 ± 0.10	5.75 ± 0.15	5.2 ± 9.2
Electrical conductivity (mS cm^{-1})	0.14 ± 0.00	0.14 ± 0.00	0.04 ± 0.14
Total dissolved solids (mg L^{-1})	0.07 ± 0.00	0.07 ± 0.00	0.02 ± 0.09

2.3 Electrode preparation

The titanium mesh was cut to size and rolled into cylinders followed by anodisation to produce self-organised TiNT. The anodising was conducted using a 2-electrode process as shown in Figure 3. The cathodes were a titanium mesh and a stainless-steel rod, the working electrode was the titanium mesh to be used in the PEC reactor. The electrolyte solution contained ethylene glycol (97 vol%), water (3 vol%) and NH_4F (0.3 wt%) in a polypropylene container as previously reported by Yeonmi et al. [30]. A potential difference of 30 V was applied for 3 hours and then washed in distilled water followed by annealing at 450ºC for 1 hour (ramp up 2°C min^{-1} up and ramp down 2°C min^{-1}). Confirmation of tube growth was done by imaging with scanning electron microscopy (SEM) (Hitachi FESEM SU5000).

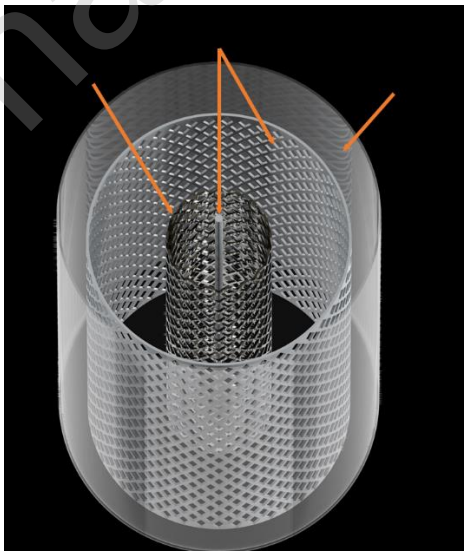

Figure 3 ± Electrode configuration for anodisation

2.4 I-V curves for different conductivities

The photocurrent-voltage (*I-V*) response was measured for different conductivities of NaCl. The solutions were made using distilled water, adjusted using NaCl and measured using a Mettler Toledo SevenEasy conductivity meter. A bias between 0 - 2 V was applied to the PEC reactor using a PLH120 DC power supply from Aim-TTi and the current was measured using a digital multimeter 1351 from Data Precision. To ensure a uniform source of irradiation a 1000 W Xe lamp was used which has an average UV intensity of 44 Wm^{-2}. All other experiments where performed under real solar conditions in South Africa.

2.5 Microbial analysis

2.5.1 Bacterial cultures

The systems were tested using two environmental Gram-negative bacterial strains, *E.coli* (S7 13) as the benchmark organism and *P. aeruginosa* (S1 68) which has been reported to have a higher resistance to solar disinfection than *E.coli* [14] and is commonly present in domestic rainwater harvesting sources [31]. The strains were obtained from the Water Resource Laboratory culture collection (Department of Microbiology, Stellenbosch University) and were previously isolated and identified by Clemente et al. [32] from untreated harvested rainwater (*E. coli* S7 13) and from rainwater following treatment > 70°C using a solar pasteurisation system (*P. aeruginosa* S1 68).

A fresh liquid culture of was prepared for each experiment, following the same produce. 200 mL of nutrient broth was inoculated with 1 colony forming unit (CFU) of the selected bacteria to be tested and incubating at 30°C for 18 hours on a rotary shaker. The inoculated broth was then centrifuged at 8000 RPM for 15 min to form a pellet. The supernatant was then discarded, and the cells were re-suspended in 50 ml of 0.85% NaCl. The optical density was measured to determine the concentration in CFU mL^{-1}, the autoclaved rainwater was then spiked to ensure D FRQFHQWUDWLRQ RI ~6 log CFU mL^{-1}. This is significantly higher than the reported concentration of *E. coli* in rainwater harvesting systems <2.5 x 10^2 CFU 100 ml^{-1} (0.4 log CFU ml^{-1}) [33]; however, the total heterotrophic bacterial counts are in the range of 3-5 log CFU ml^{-1} [34] and the WHO stipulates that for the highest level of bacterial protection a HWT system must achieved > 4 log CFU mL^{-1}; therefore an initial concentration of at least 6 log CFU mL^{-1} is required [7].

2.5.2 Enumeration of microorganisms

Water samples were collected from the reactors at set time intervals (0, 30, 60, 120, 180 and PLQXWHV6HULDOGLOXWLRQVZKHUHPDGHXVLQJ1D&ODQG/ZDVVSUHDGSODWHGRQ nutrient agar in duplicate. The plates for both microorganisms were incubated at 37^{o}C overnight (18 h) and the CFU was enumerated. The results of enumeration are expressed as the average CFU mL^{-1} for each sample time and deviation of all data shown using error bars. When low counts of bacteria were expected, plating with no dilution was performed using 100 /WKXVJLYLQJDGHWHFWLRQOLPLW RI &)8P/ (1 $\log_{10}$).

2.5.3 Viability analysis using EMA-qPCR

Ethidium monoazide bromide (EMA) is a nucleic acid-binding dye that can be used as a pre-treatment step before quantitative real-time polymerase chain reaction (qPCR) to assess the YLDELOLW\RIEDFWHULDEDVHGRQWKHFHOO¶VPHPEUDQHLQWHJULW\,IWKHLQWHJULW has been affected during the treatment process, EMA will bind to the DNA and will prevent amplification of the bound DNA during qPCR; the DNA from cells with intact membranes will however amplify [35].

EMA-qPCR was performed on each sample taken from the reactors. The samples were treated with EMA following the method described by Reyneke et al. [36]. To summarise 2.5 µg ml^{-1} of EMA was added to 1 ml of sample in a dark room, vortexed and left on ice for 10 min, followed by a 15 min 500W halogen lamp exposure (Eurolux, South Africa) enabling the photosensitive EMA to crosslink with the DNA. Following photoactivation, 1 ml of 0.85% NaCl was added to the sample, vortexed and centrifuged at 16,000 RCF for 5 min. The supernatant was then removed and DNA extraction performed using the *Quick*-16S Faecal/Soil Microbe Miniprep Kit IROORZLQJ WKH PDQXIDFWXUHU¶V LQVWUXFWLRQV 7KH reaction mixture, quantification curve and procedures as reported by Waso et al. [34] was used. Briefly, the qPCR reaction mixture (20 µL) contained: 10 µL FastStart Essential DNA Green Master Mix, 5 µL of template DNA, 0.4 µL (0.2 µM) forward and reverse genus-specific primers and 4.2 µL of PCR-grade water. The qPCR primers and cycling parameters are shown in Table 2. Melt curve analysis was included for all qPCR assays in order to verify the specificity of the primer set by ramping the temperature from 65 to 97°C at a rate of 0.2°C s^{-1} with continuous fluorescent signal acquisition at 5 readings °C^{-1}. To prepare the standard curves for the quantification of *E. coli* and *P. aeruginosa*, DNA (positive control DNA) was

extracted from pure cultures using the *Quick*-'1$)DHFDO6RLO 0LFUREH 0LQLSUHS .LW DFFRUGLQJWRWKHPDQXIDFWXUHU¶VLQVWUXFWLRQV The obtained DNA was amplified in conventional PCR reactions using the primers and cycling parameters outlined in Table 2, whereafter the amplicons were purified and concentrated using the Wizard® SV Gel and PCR Clean-up 6\VWHP3URPHJDDFFRUGLQJWRWKHPDQXIDFWXUHU¶VLQVWUXFWLRQV)ROORZLQJ'1$FRQFH determination using a NanoDrop® ND-1000 (Nanodrop Technologies Inc.), the DNA concentration and gene product size were then used to calculate the dilution required to obtain a final DNA concentration of 10^9 JHQH FRSLHV *&/ $^{-1}$ and 10-fold serial dilutions were prepared (10^9 GC µL^{-1} to 10^0 GC µL^{-1}). All qPCR was performed on a LightCycler®96 instrument (Roche Applied Science Mannheim, Germany) and analysed using LightCycler®96 software version 1.1.

Table 2 ± Primers and cycling parameters utilised for GC quantification for *E. coli* and *Pseudomonas spp.*

Organism	Primer	Primer Sequence	qPCR cycling Parameters	Target Gene & Product Size (Base Pairs)	Reference
E. coli	784 F	GTGTGATATCTA CCCGCTTCGC	10 min at 95°C; 30 cycles of 95°C for 15s, 60°C for 1 min, final elongation at 72°C for 10 min	*uidA* gene (80 bp)	[37]
	866 R	AGAACGGTTTGT GGTTAATCAGGA			
Pseudomonas spp.	PS1	ATGAACAACGTT CTGAAATTC	*PLQDW* *HRV* *DW* *QGVDW* 72°C	*oprI* gene (249 bp)	[38]
	PS2	CTGCGGCTGGCT TTTTCCAG			

The samples were analysed in duplicate and the average GC concentrations were used. The detection limit was calculated from the quantification curve, using the average of the lowest level of detection; each qPCR run uses a new quantification curve thus the DL varies based on the lowest value of the curve. The GC values were converted from GC µL^{-1} to GC 100 mL^{-1} original sample using the equation by Rajal et al. [39] (Eq. 1).

• ”‹‰‹•ƒŽ•ƒ‰’Ž‡ ”‡ƒ…–‹‘•

@ kPSpgegW_jknjJgjrcpcb / kPEdrcJgjrp_rgml Aš @ kPYqcb lHRE vrp_rgmJ / QjHRE jsrcb Aš • ’‡”“ (1)

3. Results

3.1 Electrode characterisation

Following anodisation the TiNT were analysed using SEM as shown in Figure 4.

Figure 4 ± a) showing the alignment of the tube, b) length of TiNT, c) flat area used to analyse tube diameter, d) histogram of tube diameter

The SEM images showed coverage of the highly ordered nanotubes across the surface of the material. As shown in Figure 4a, the tubes appear to change orientation from one side to the other of the sample. This could be attributed to the changing surface geometry relative to the electron beam and/or changes in local electric field when anodising due to the changing tangent of the cylindrical electrodes and therefore changing the direction of tube growth [40]. Figure 4b and Figure 4c were used to measure the length and diameter of the nanotubes respectively. The length of the nanotubes were between 2.37 ± 2.52 µm and the average diameter of the nanotubes was 92 nm with a standard deviation of 9.9 from a sample size of 65. A histogram of the nanotubes size distribution is shown in Figure 4d; it shows a normal distribution pattern.

The length and size of the nanotubes are comparable to others reported when anodising at 30V for 3 hours [41, 42].

3.2 Photocurrent response for different conductivities

The optimal cell potential reported in literature for TiO_2 electrodes changes depending upon the reactor geometry and set-up, the conductivity/electrolyte of the solution and the target contaminates [43, 44]. As expected, the photocurrent increases with decreasing solution resistance and the bias at which photocurrent saturation begins, also decreases (Figure 5). The bias used for disinfection was 1.0 V, which has been a commonly reported potential when running PEC systems [45-47]. This is close to the potential for maximum photocurrent with the rainwater conductivity of 70 μScm^{-1}. Pablos et al. [47] had improved disinfection results with a cell potential of 1.4 V compared to 1 V but the optimum applied potential required will depend on the cell resistance. It should also be noted that there is not a direct relationship between the photocurrent and the rate of disinfection when comparing different photoanode materials: However, for any one photoanode, the maximum photocurrent is a measure of maximum charge carrier separation and, therefore, should correlate to the maximum rate of disinfection [19].

Figure 5 ± *I-V* curve of the PEC reactor

3.3 Correlation of photocurrent and UV intensity

The photocurrent was recorded and correlated to the UV intensity. As taking samples from the reactor reduced the volume and surface area of electrodes in contact with the solution there was a reduction in the current, to account for this the current was adjusted by multiplying the current by the ratio of the volume reduction (original volume/volume remaining after taking sample).

The current changes as the UV intensity changes during the experiment as shown in Figure 6a. Plotting a graph of the adjusted current with respect to UV intensity shows a linear correlation (Figure 6b). The correlation is mathematically expressed in Eq. 2.

Figure 6 ± a) UV (280±400 nm) data and current data from PEC reactor, b) correlation between UV radiation and recorded current data

: • ?6; L $\frac{\text{X m r Gjs p p c?lH\_ pG s p r c l r}}{\text{W w q r Gkm l q r \_ 46 :}}$ (2)

3.4 Enumeration and viability of E. coli & P. aeruginosa

The rainwater disinfection experiment for *E. coli* was performed under real sun radiation during winter (high rainfall period in South Africa). Experiments were duplicated and the average UV (280-400 nm) irradiance on the two days was 10.8 W m^{-2} and 11.2 W m^{-2}, (3.6% difference). The data in Figure 7 (a) shows the average between the repeat experiments. There was a significant increase in the rate of inactivation of *E.coli* with the PEC system operating at 1.0 V in comparison to the photo-inactivation alone (Figure 7a). With the PEC reactor, a 5.5 log reduction of *E. coli* CFU ml^{-1} was observed in 4 h of irradiation as compared to a 3.1 log reduction for photo-inactivation. As *E. coli* may still be viable but in a nonculturable state after the EAP treatment [48], viability analysis was used, applying the EMA-qPCR method (Figure 7b). The results clearly showed that the damage produced by the mere action of the solar radiation had a very limited effect on the cell membrane, as only a small 0.45 log reduction in the *E. coli* GC concentration was recorded in 4 hours of solar treatment (using only photo-inactivation) (Figure 7b). In contrast, the PEC reactor yielded a 2.4 log reduction in the *E. coli*

GC (Figure 7b), indicating that the cell membrane had been damaged and a larger quantity of the bacteria were no longer viable.

Figure 7 ± a) Culture-based analysis for the reduction in *E. coli* and UV irradiation. The data points are the average from two experiments where the error is the standard deviation (including analytical and experimental) and the UV is the average, b) EMA-qPCR gene copies (analytical error only). (UV = 280-400 nm, UVB = 280-315 nm)

For the disinfection tests with spiked *P. aeruginosa* the average UV irradiance on the two days was 13.3 W m^{-2} and 10.7 W m^{-2}. The culture based analysis results (Figure 8a) showed a 2.7 log reduction in *P. aeruginosa* for photo-inactivation after 1 h of irradiation and no further reduction was observed during the experiment, indicating that *P. aeruginosa* is more resistant to solar photo-inactivation consistent with previous reports [49]. In the PEC reactor, a total reduction of 5.8 log was observed. Molecular viability analysis for *P. aeruginosa* using EMA-qPCR (Figure 8b) indicated a 0.91 log reduction of GC for photo-inactivation as compared to a 3 log reduction with PEC, reaching the detection limit.

Figure 8 ± a) - Culture-based analysis for the reduction in *P. aeruginosa* and UV irradiation. The data points are the average from two experiments where the error is the standard deviation (including analytical and experimental) and the UV is the average, b) EMA-qPCR gene copies. (analytical error only). (UV = 280-400 nm, UVB = 280-315 nm).

4. Discussion

The application of viability dyes, and specifically EMA, in combination with qPCR to detect viable cells has been proven to be effective for certain Gram-positive (*E. faecalis*) and Gram-negative organisms (*P. aeruginosa and S. typhimurium*) [50]. Moreover, the use of the same technique to distinguish between live and dead cells was used by Polo-Lopez et al. [51] for the detection of *Legionella jordanis* in water [51]. The EMA-qPCR method was used in the current study to distinguish between live and dead bacterial cells as it effectively suppresses the signal from extracellular DNA or internal DNA from cells with damaged membranes. However, it may also pass through the intact membrane of live cells or even be cytotoxic to viable cells in high concentrations [35]. Therefore, while it is a very good method to establish the viability of microbial cells, adequate concentrations of the viability dye have to be applied in order to obtain reliable results. An EMA-qPCR method optimised by Reyneke et al. [50] was thus used in the current study for the detection of the two test organisms.

In this work, the disinfection experiments compare two different processes i.e., solar photo-inactivation and the solar driven EAP disinfection. Both produce either lethal or sublethal damage to bacterial cells via different mechanisms. Photo-inactivation relies on the absorption

of solar UV photons by several components of the bacteria called chromophores. UVB causes DNA damages resulting from its direct absorption by DNA, effectively preventing its replication or producing mutations [52]. Other mechanisms are recognised as responsible for the microbial inactivation, which include the direct absorption of UVA radiation by DNA, and the oxidative attacks of internal ROS generated by the absorption of UVA radiation by internal chromophores [53]. The photogenerated ROS can damage the DNA producing single strand breaks, lead to the formation of pyrimidine dimers, oxidise proteins and lipids, or produce losses in the permeability of the cell membrane compromising cells [54]. Research investigating solar inactivation shows a high reduction in CFU of >4 log for *E. coli*; which is classified as highly protective in terms of bacterial reduction by the WHO [55, 56]. In this research, a lower reduction of 3.1 log CFU ml^{-1} for *E. coli* was observed using photo-inactivation. This could be due to the low dose of solar UV radiation (280-400 nm) which amounted to 161.3 kJm^{-2} and the use of environmental bacterial isolates, which could be more resistant to solar inactivation as compared to traditionally used laboratory strains [13]. The work of Cruz-Ortiz et al. [57] reported a slightly higher reduction of 3.6 log for *E.coli*, for photo-inactivation using a solar simulated source with a much higher UV dose of 574.4 kJm^{-2}. The experiments in this work were however, conducted under real sun during winter days in South Africa with low UV intensity values, ca. 16% lower than a normal sunny day in a moderate latitude with air mass of 1.5. The solar inactivation of *P. aeruginosa* in this work resulted in 2.7 log CFU ml^{-1} reduction after receiving a cumulative dose of 155.0 kJm^{-2} during the 4-hour experiment. *P. aeruginosa* is less commonly reported as a model organism for solar disinfection but more resilient than *E. coli*. The reported UV dose for a 5 log reduction is 1440 kJ m^{-2} under simulated solar irradiation [58] and the dose for a 1 log reduction has been reported to be 72 kJ m^{-2} under real solar conditions [13]. The latter correlates closely to the result obtained in this study. At sub-lethal doses of UV, bacteria have the ability to repair their damaged DNA [59]. Photoreactivation uses the photolyase enzyme to repair the damaged DNA, which requires wavelengths between 300-500 nm (present in solar irradiation) [60]. Nucleotide excision repair is an important repair mechanism after the exposure to UV. It is a complex multiple step non-light dependent biochemical process requiring a number of different enzymes [61]. Therefore, it is difficult to provide quality assurance for solar photo-inactivation alone due to daily variations in solar irradiance and different resistance and repair mechanisms of naturally occurring bacteria.

Solar driven EAP disinfection requires a more complicated reactor but resulted in greater and more effective inactivation of bacteria, with a 5.5 log reduction of *E. coli* CFU ml^{-1} observed in 4 h and a 5.8 log reduction in *P. aeruginosa* CFU ml^{-1} recorded. Higher EMA-qPCR inactivation efficiencies were also obtained for both test organisms using the EAP reactor in comparison to simple photo-inactivation. This is due to the combined effect of photo-inactivation and reactive oxygen species formed through electrochemically assisted photocatalysis. Under irradiation, the TiO_2 nanotube electrode producHV K\GUR[\O UDGLFDO¶V (‡2+ which have a very positive electrochemical reduction potential of +2.18 V (NHE at pH 7) but has a short lifetime of <40 µs resulting in a short diffusion length of 1.4 nm [22, 62]. The ‡2+ is the main radical reported for disinfection, however there are other pathways responsible for disinfection. The ‡2+FDQUHDFWZLWKRWKHUVSHFLHVSUHVHQWLQUDLQZDWHU bicarbonate (HC2) to form carbonate radical (C2 ?) which has a longer lifetime of ~8 ms, but a lower oxidation potential (1.59 V vs NHE pH 7) than the ‡2+ . It is capable of oxidising guanine (1.29 V vs NHE) and has been shown to inactivate *E. coli* and MS2 coliphages [63, 64]. Rainwater also contains small amounts of chloride (Cl-) in the range of 19 - 322 µeq L-1 depending on the geographical region [65]. Chloride can be oxidised to form reactive chlorine species (RCS), such as chloride radicals and chorine which contribute to the inactivation of microorganisms [65].

At the cathode side, the one electron reduction of oxygen leads to the production of superoxide (2 ?) or hydroperoxyl radical (HOO‡)XUWKHURQHHOHFWURQUHGXFWLRQUHVXOWVLQK\GU peroxide (H_2O_2), which can be further reduced to form OH radicals. Unmodified carbon felt was used as a cathode in this reactor. Carbon can act as an electrocatalyst for the selective reduction of dissolved O_2 to produce H_2O_2 [21, 66-68]. Subsequent one electron reduction of H_2O_2 yields ‡2+DWWKHFDWKRGH. The cathode may be further enhanced for the production of H_2O_2 by using electrocatalysts. The work of Sun et al. [68] used modified mesoporous carbon which exhibited high selectively towards H_2O_2 and improved yield.

The conductivity of the water will have a significant effect on the current as shown in Figure 5. By Faradays law, increasing the current will increase the number of ROS, provided the efficiency remains the same [69]. However, with increased conductivity there are more ions that will scavenge ‡OH and the increased ionic strength reduces the electrophoretic mobility of bacteria [70]. Therefore, the relationship between ionic strength, photocurrent and disinfection rate is not a simple one. Cho et al. [17] used a particulate film of TiO_2 immobilised on indium

tin oxide coated glass the photoanode with a stainless steel counter electrode back faced irradiated with a UV lamp. The authors demonstrated that increasing the conductivity using phosphate buffer up to 40 mM (estimated to be ~6 $mScm^{-1}$) improved the rate of disinfection of MS2 coliphages, while increasing further to 60 mM (estimated to be ~9 $mScm^{-1}$) resulted in ORQJHUWLPHVWRDFKLHYHDORJUHGXFWLRQ7KH\DOVRUHSRUWHGWKDWKLJKFXUUHQ result in a high rate of disinfection, because of electro-osmotic repulsion of the MS2 coliphage away from the photoanode where WKH IRUPDWLRQ RI VXUIDFH l^{3+} SUHVLGHV WKH PDLQ UDGL responsible for the inactivation of MS2 coliphages. Pablos et al. [47] tested for the inactivation of *E. coli* using 100 mM Na_2SO_4 (16 $mScm^{-1}$) and synthetic municipal wastewater (0.04 $mScm^{-1}$), both of which resulted in a similar rate of disinfection indicating that very high and very low conductivities are suboptimal. Koo et al. [65] tested for the disinfection of *E. coli* using 100 mM Na_2SO_4 (16 $mScm^{-1}$) in a saline solution. Results indicated that the addition of the 50 mM of NaCl improved the rate of disinfection due to the oxidation of chloride forming RCS as discussed previously. Therefore, the nature and concentration of ions present in the water will have a significant effect on the rate of EAP disinfection. To summarise, the presence of chloride ions is beneficial for inactivation as RCS can be formed. Increased ionic strength will yield higher photocurrent due to lower cell resistance. Increased photocurrent should yield more ROS but the increased ionic strength means there are more ions to scavenge the ROS. As ionic strength increases, the electrophoretic mobility of microorganisms towards the photoanode is decreased. Accordingly, there is an optimal conductivity based on the work of Cho et al. [17] around 6 mS cm^{-1} which results in the best rate for disinfection but that will also be dependent on the nature of the ions in solution. However, for the disinfection of harvested rain water for potable use it is not desirable to add salts to increase the conductivity and the results of this work demonstrate that solar EAP can effectively disinfect harvested rain water, without adulteration.

5. Conclusions

Culture-based and viability-based methods were used to evaluate the performance of a PEC reactor using a mesh photoanode with self-organised TiNT, tested using solar irradiation with a low average UV intensity (10.7 ± 13.3 Wm^{-2}) for the disinfection for both *E. coli* and *P. aeruginosa* in low conductivity rainwater (70 $PScm^{-1}$). The PEC reactor demonstrated significant improvement in reduction of both organisms compared to photo-inactivation alone. For culture-based methods the PEC reactor achieved an averaged 5.5 log reduction for *E. coli*

and 5.8 log reduction in *P. aeruginosa*. The viability-based methods show that the organisms could potentially still be viable when using only solar photo-inactivation. The PEC also had significantly improved results when monitoring the system using molecular-based viability methods that may account for the presence of viable but non-culturable cells, with a 2.4 log reduction for *E. coli* and 3.0 log reduction in *P. aeruginosa* recorded. While a PEC reactor is more complicated and more costly than a solar disinfection reactor, it will provide a faster and more effective disinfection treatment, particularly for organisms which have a greater resistance to photo-inactivation. The use of EAP reactors for the disinfection of water still needs further improvements which could be accomplished by modelling the reactors, using thin cell reactors to reduce IR losses/improve mass transport, devolvement into a flow set-up to treat larger volumes, the use of electrocatalysts on the cathode such as mesoporous nitrogen doped carbon, improvements in the efficiency of photoanode by utilising visible light and critical analysis of possible disinfection by-products.

Author contributions

S. McMichael: Conceptualisation, Investigation, Writing - Original Draft, Writing - review & editing. **M. Waso**: Methodology and Writing - review & editing. **B. Reyneke**: Methodology and Writing - review & editing. **W. Khan**: Funding acquisition, Supervision, Methodology, Writing - review & editing. **P. Fernandez Ibanez**: Funding acquisition, Supervision, Writing - review & editing. **J.A. Byrne**: Funding acquisition, Supervision, Writing - review & editing

Declaration of Competing Interest

The authors declare that they have no known competing financial interests or personal relationships that could have appeared to influence the work reported in this paper.

Acknowledgments

The authors wish to acknowledge the Department for Economy (DfE) Northern Ireland for funding Stuart McMichael, the Global Challenges Research Fund (GCRF) UK Research and Innovation for funding SAFEWATER (Grant Reference EP/P032427/1) and the Royal Society for funding the Newton Mobility Grant award (NI170184).

References

[1] T.I.E. Veldkamp, Y. Wada, H. de Moel, M. Kummu, S. Eisner, Aerts, Jeroen C. J. H., P.J. Ward, Changing mechanism of global water scarcity events: Impacts of socioeconomic changes and inter-annual hydro-climatic variability, Global Environ Chang. 32 (2015) 18-29. https://doi.org/10.1016/j.gloenvcha.2015.02.011.

[2] United Nations, The Sustainable Development Goals Report 2017, UN, New York, 2017

[3] M. Semaan, S.D. Day, M. Garvin, N. Ramakrishnan, A. Pearce, Optimal sizing of rainwater harvesting systems for domestic water usages: A systematic literature review, Resources, Resour Conserv Recycl 6 (2020) 100033. https://doi.org/10.1016/j.rcrx.2020.100033.

[4] A. Sharma, D. Begbie, T. Gardner, Rainwater Tank Systems for Urban Water Supply, IWA, London, UK, 2015.

[5] W. Ahmed, T. Gardner, S. Toze, Microbiological quality of roof-harvested rainwater and health risks: A review, J. Environ. Qual. 40 (2011) 13-21. https://doi.org/10.2134/jeq2010.0345.

[6] World Health Organization, Guidelines for Drinking-Water Quality: Fourth Edition Incorporating First Addendum, 4th ed + 1st addendum ed., World Health Organization, Geneva, 2017.

[7] World Health Organization, Results of Round I of the WHO International Scheme to Evaluate Household Water Treatment Technologies (2016). World Health Organization, Geneva, 2016

[8] B.K. Mishra, S.K. Gupta, A. Sinha, Human health risk analysis from disinfection by-products (DBPs) in drinking and bathing water of some Indian cities, J. Enviorn. Health Sci. Eng. 12 (2014). https://doi.org/10.1186/2052-336X-12-73.

[9] A. Omarova, K. Tussupova, R. Berndtsson, M. Kalishev, K. Sharapatova, Protozoan parasites in drinking water: A system approach for improved water, sanitation and hygiene in developing countries, Int. J. Environ. Res. Public Health. 15 (2018). https://doi.org/10.3390/ijerph15030495.

[10] K.G. McGuigan, R.M. Conroy, H.-. Mosler, M. du Preez, E. Ubomba-Jaswa, P. Fernandez-Ibañez, Solar water disinfection (SODIS): A review from bench-top to roof-top, J. Hazard. Mater. 235-236 (2012) 29-46. https://doi.org/10.1016/j.jhazmat.2012.07.053.

[11] M. Castro-Alférez, M.I. Polo-López, P. Fernández-Ibáñez, Intracellular mechanisms of solar water disinfection, Sci. Rep. 6 (2016). https://doi.org/10.1038/srep38145.

[12] M. Fontán-Sainz, H. Gómez-Couso, P. Fernández-Ibáñez, E. Ares-Mazás, Evaluation of the solar water disinfection process (SODIS) against Cryptosporidium parvum using a 25-L static solar reactor fitted with a Compound Parabolic Collector (CPC), Am. J. Trop. Med. Hyg. 86 (2012) 223-228. https://doi.org/10.4269/ajtmh.2012.11-0325.

[13] S. Dejung, I. Fuentes, G. Almanza, R. Jarro, L. Navarro, G. Arias, E. Urquieta, A. Torrico, W. Fenandez, M. Iriarte, C. Birrer, W.A. Stahel, M. Wegelin, Effect of solar water disinfection (SODIS) on model microorganisms under improved and field SODIS conditions, J. Water Supply Res. Technol. Aqua. 56 (2007) 245-256. https://doi.org/10.2166/aqua.2007.058.

[14] J.A. Byrne, P.S.M. Dunlop, J.W.J. Hamilton, P. Fernández-Ibáñez, I. Polo-López, P.K. Sharma, A.S.M. Vennard, A review of heterogeneous photocatalysis for water and surface disinfection, Molecules. 20 (2015) 5574-5615. https://doi.org/10.3390/molecules20045574.

[15] Y. Abdel-Maksoud, E. Imam, A. Ramadan, TiO_2 solar photocatalytic reactor systems: Selection of reactor design for scale-up and commercialization² analytical review, Catalysts. 6 (2016). https://doi.org/10.3390/cata6090138.

[16] M.F.J. Dijkstra, A. Michorius, H. Buwalda, H.J. Panneman, J.G.M. Winkelman, Beenackers, A. A. C. M., Comparison of the efficiency of immobilized and suspended systems in photocatalytic degradation, Catal. Today. 66 (2001) 487-494. https://doi.org/10.1016/S0920-5861(01)00257-7.

[17] M. Cho, F.L. Cates, J.-. Kim, Inactivation and surface interactions of MS-2 bacteriophage in a TiO_2 photoelectrocatalytic reactor, Water Res. 45 (2011) 2104-2110. https://doi.org/10.1016/j.watres.2010.12.017.

[18] P.S.M. Dunlop, J.A. Byrne, N. Manga, B.R. Eggins, The photocatalytic removal of bacterial pollutants from drinking water, J. Photochem. Photobiol. A. 148 (2002) 355-363. https://doi.org/10.1016/S1010-6030(02)00063-1.

[19] C. Pablos, J. Marugán, R. Van Grieken, P.S.M. Dunlop, J.W.J. Hamilton, D.D. Dionysiou, J.A. Byrne, Electrochemical enhancement of photocatalytic disinfection on aligned TiO_2 and nitrogen doped TiO_2 nanotubes, Molecules. 22 (2017). https://doi.org/10.3390/molecules22050704.

[20] E.I. Cedillo-Gonzalez, M. Montorsi, C. Mugoni, M. Montorsi, C. Siligardi, Improvement of the adhesion between TiO_2 nanofilm and glass substrate by roughness modifications, Phys. Procedia. 40 (2013) 19-29. https://doi:10.1016/j.phpro.2012.12.003

[21] P. Ma, H. Ma, A. Galia, S. Sabatino, O. Scialdone, Reduction of oxygen to H_2O_2 at carbon felt cathode in undivided cells. Effect of the ratio between the anode and the cathode surfaces and of other operative parameters, Sep. Purif. Technol. 208 (2019) 116-122. https://doi.org/10.1016/j.seppur.2018.04.062.

[22] J.M. Burns, W.J. Cooper, J.L. Ferry, D.W. King, B.P. DiMento, K. McNeill, C.J. Miller, W.L. Miller, B.M. Peake, S.A. Rusak, A.L. Rose, T.D. Waite, Methods for reactive oxygen species (ROS) detection in aqueous environments, Aquatic Sci. 74 (2012) 683-734. https://doi.org/10.1007/s00027-012-0251-x.

[23] C.B. Lineback, C.A. Nkemngong, S.T. Wu, X. Li, J.J. Teska, H.F. Oliver, Hydrogen peroxide and sodium hypochlorite disinfectants are more effective against Staphylococcus aureus and Pseudomonas aeruginosa biofilms than quaternary ammonium compounds, Antimicrobial resistance and infection control. 7 (2018) 154. https://doi.org/10.1186/s13756-018-0447-5.

[24] C. Jungfer, T. Schwartz, U. Obst, UV-induced dark repair mechanisms in bacteria associated with drinking water, Water Res. 41 (2007) 188-196. https://doi.org/10.1016/j.watres.2006.09.001.

[25] Q. Wang, L. Wang, R. Tang, Design and Optical Performance of Compound Parabolic Solar Concentrators with Evacuated Tube as Receivers, Energies. 9 (2016) 795. https://doi.org/10.3390/en9100795.

[26] C. Navntoft, E. Ubomba-Jaswa, K.G. McGuigan, P. Fernández-Ibáñez, Effectiveness of solar disinfection using batch reactors with non-imaging aluminium reflectors under real conditions: Natural well-water and solar light, J Photoch Photobio B. 93 (2008) 155-161. https://doi.org/10.1016/j.jphotobiol.2008.08.002.

[27] P. Fernández, J. Blanco, C. Sichel, S. Malato, Water disinfection by solar photocatalysis using compound parabolic collectors, Catal. Today. 101 (2005) 345-352. https://doi.org/10.1016/j.cattod.2005.03.062.

[28] L.C. Navntoft, P. Fernandez-Ibañez, F. Garreta, UV solar radiation on a tilted and horizontal plane: Analysis and comparison of 4years of measurements, Sol. Energy. 86 (2012) 307-318. https://doi.org/10.1016/j.solener.2011.10.004.

[29] B. Reyneke, T. Ndlovu, M.B. Vincent, A. Martínez-García, M.I. Polo-López, P. Fernández-Ibáñez, G. Ferrero, S. Khan, K.G. McGuigan, W. Khan, Validation of large-volume batch solar reactors for the treatment of rainwater in field trials in sub-Saharan Africa, Sci. Total Environ. 717 (2020). https://doi.org/10.1016/j.scitotenv.2020.137223.

[30] S. Yeonmi, L. Seonghoon, Self-organized regular arrays of anodic TiO2 nanotubes, Nano Lett. 8 (2008) 3171-3173. https://doi.org/10.1021/nl801422w.

[31] M.T. Amin, M. Nawaz, M.N. Amin, M. Han, Solar Disinfection of *Pseudomonas* aeruginosa in Harvested Rainwater: A Step towards Potability of Rainwater, PloS one. 9 (2014) e90743. https://doi.org/10.1371/journal.pone.0090743.

[32] T. Clements, B. Reyneke, A. Strauss, W. Khan, Persistence of Viable Bacteria in Solar Pasteurised Harvested Rainwater, Water Air Soil Pollut. 230 (2019). https://doi.org/10.1007/s11270-019-4164-z.

[33] P. H. Dobrowsky, A. van Deventer, M. De Kwaadsteniet, T. Ndlovu, S. Khan, T. E. Cloete, W. Khan, Prevalence of Virulence Genes Associated with Pathogenic Escherichia coli Strains Isolated from Domestically Harvested Rainwater during Low- and High-Rainfall Periods, Appl. Environ. Microbiol. 80 (2014) 1633-1638. https://doi.org/10.1128/AEM.03061-13.

[34] M. Vaso, S. Khan, W. Khan, Microbial source tracking markers associated with domestic rainwater harvesting systems: Correlation to indicator organisms, Environ. Res. 161 (2018) 446-455. https://doi.org/10.1016/j.envres.2017.11.043.

[35] M. Fittipaldi, A. Nocker, F. Codony, Progress in understanding preferential detection of live cells using viability dyes in combination with DNA amplification, J. Microbiol. Methods. 91 (2012) 276-289. https://doi.org/10.1016/j.mimet.2012.08.007.

[36] B. Reyneke, P.H. Dobrowsky, T. Ndlovu, S. Khan, W. Khan, EMA-qPCR to monitor the efficiency of a closed-coupled solar pasteurization system in reducing Legionella contamination of roof-harvested rainwater, Sci. Total Environ. 553 (2016) 662-670. https://doi.org/10.1016/j.scitotenv.2016.02.108.

[37] E. Frahm, U. Obst, Application of the fluorogenic probe technique (TaqMan PCR) to the detection of *Enterococcus spp*. and *Escherichia coli* in water samples, J. Microbiol. Methods. 52 (2003) 123-131. https://doi.org/10.1016/S0167-7012(02)00150-1.

[38] L. Bergmark, P.H.B. Poulsen, W.A. Al-Soud, A. Norman, L.H. Hansen, S.J. Sørensen, Assessment of the specificity of *Burkholderia* and *Pseudomonas* qPCR assays for detection of these genera in soil using 454 pyrosequencing, FEMS Microbiol. Lett. 333 (2012) 77-84. https://doi.org/10.1111/j.1574-6968.2012.02601.x.

[39] V.B. Rajal, B.S. McSwain, D.E. Thompson, C.M. Leutenegger, S. Wuertz. Molecular quantitative analysis of human viruses in California stormwater, Water Res. 41 (2007) 4287-4298. https://doi.org/10.1016/j.watres.2007.06.002.

[40] B. Yin, Q. Qian, Z. Xiong, H. Jiang, Y. Lin, D. Feng, Growth orientation mechanism of TiO2 nanotubes fabricated by anodization, Nanotechnology. 30 (2019). https://doi.org/10.1088/1361-6528/aafd54.

[41] S. Li, S. Lin, J. Liao, N. Pan, D. Li, J. Li, Nitrogen-doped TiO_2 nanotube arrays with enhanced photoelectrochemical property, Int. J. Photoenergy. 2012 (2012). https://doi.org/10.1155/2012/794207.

[42] C. Adán, J. Marugán, E. Sánchez, C. Pablos, R. van Grieken, Understanding the effect of morphology on the photocatalytic activity of TiO2 nanotube array electrodes, Electrochim. Acta. 191 (2016) 521-529. https://doi.org/10.1016/j.electacta.2016.01.088.

[43] A. Pirkarami, M.E. Olya, S. Raeis Farshid, UV/Ni±TiO2 nanocatalyst for electrochemical removal of dyes considering operating costs, Water Resour. Ind. 5 (2014) 9-20. https://doi.org/10.1016/j.wri.2014.02.001.

[44] E. Zarei, Electrochemically assisted photocatalytic removal of m-cresol using TiO_2 thin film-modified carbon sheet photoelectrode, Int. J. Ind. Chem. 9 (2018) 285-294. https://doi.org/10.1007/s40090-018-0158-z.

[45] J. Bai, Y. Liu, J. Li, B. Zhou, Q. Zheng, W. Cai, A novel thin-layer photoelectrocatalytic (PEC) reactor with double-faced titania nanotube arrays electrode for effective degradation of tetracycline, Appl. Catal. B. 98 (2010) 154-160. https://doi.org/10.1016/j.apcatb.2010.05.024.

[46] K. Cho, S. Lee, H. Kim, H. Kim, A. Son, E. Kim, M. Li, Z. Qiang, S.W. Hong, Effects of reactive oxidants generation and capacitance on photoelectrochemical water disinfection with self-doped titanium dioxide nanotube arrays, Appl. Catal. B. 257 (2019) 117910. https://doi.org/10.1016/j.apcatb.2019.117910.

[47] C. Pablos, J. Marugán, C. Adán, M. Osuna, R. van Grieken, Performance of TiO_2 photoanodes toward oxidation of methanol and *E. coli* inactivation in water in a scaled-up photoelectrocatalytic reactor, Electrochim. Acta. 258 (2017) 599-606. https://doi.org/10.1016/j.electacta.2017.11.103.

[48] M. Ben Said, O. Masahiro, A. Hassen, Detection of viable but non cultivable *Escherichia coli* after UV irradiation using a lytic Qß phage, Ann. Microbiol. 60 (2010) 121-127. https://doi.org/10.1007/s13213-010-0017-4.

[49] J. Rodriguez-Chueca, M. Morales, R. Mosteo, M.P. Ormad, J.L. Ovelleiro, Inactivation of *Enterococcus faecalis, Pseudomonas aeruginosa* and *Escherichia coli* present in treated urban wastewater by coagulation-flocculation and photo-Fenton processes, Photoch Photobio Sci. 12 (2013) 864-871. https://doi.org/10.1039/c3pp25352j.

[50] B. Reyneke, T. Ndlovu, S. Khan, W. Khan, Comparison of EMA-, PMA- and DNase qPCR for the determination of microbial cell viability, Appl. Microbiol. Biotechnol. 101 (2017) 7371-7383. https://doi.org/10.1007/s00253-017-8471-6.

[51] M.I. Polo-López, M. Castro-Alférez, S. Nahim-Granados, S. Malato, P. Fernández-Ibáñez, Legionella jordanis inactivation in water by solar driven processes: EMA-qPCR versus culture-based analyses for new mechanistic insights, Catal. Today. 287 (2017) 15-21. https://doi.org/10.1016/j.cattod.2016.10.029.

[52] R.P. Sinha, D. Häder, UV-induced DNA damage and repair: a review, Photoch Photobio Sci. 1 (2002) 225-236. https://doi.org/10.1039/b201230h.

[53] R.M. Tyrrell, S.M. Keyse, New trends in photobiology the interaction of UVA radiation with cultured cells, J. Photoch. Photobio. B. 4 (1990) 349-361. https://doi:10.1016/1011-1344(90)85014-N.

[54] M. Berney, H. Weilenmann, T. Egli, Flow-cytometric study of vital cellular functions in *Escherichia coli* during solar disinfection (SODIS), Microbiology. 152 (2006) 1719-1729. https://doi.org/10.1099/mic.0.28617-0.

[55] World Health Organization, Evaluating Household Water Treatment Options: Health-based targets and microbiological performance specifications (2011), World Health Organization, Geneva

[56] R. Nalwanga, B. Quilty, C. Muyanja, P. Fernandez-Ibañez, K.G. McGuigan, Evaluation of solar disinfection of *E. coli* under Sub-Saharan field conditions using a 25L borosilicate glass batch reactor fitted with a compound parabolic collector, Sol. Energy. 100 (2014) 195-\202. https://doi.org/10.1016/j.solener.2013.12.011.

[57] B.R. Cruz-Ortiz, J.W.J. Hamilton, C. Pablos, L. Díaz-Jiménez, D.A. Cortés-Hernández, P.K. Sharma, M. Castro-Alférez, P. Fernández-Ibañez, P.S.M. Dunlop, J.A. Byrne, Mechanism of photocatalytic disinfection using titania-graphene composites under UV and visible irradiation, Chem. Eng. 316 (2017) 179-186. https://doi.org/10.1016/j.cej.2017.01.094.

[58] J. Lonnen, S. Kilvington, S.C. Kehoe, F. Al-Touati, K.G. McGuigan, Solar and photocatalytic disinfection of protozoan, fungal and bacterial microbes in drinking water, Water Res. 39 (2005) 877-883. https://doi.org/10.1016/j.watres.2004.11.023.

[59] J.L. Zimmer, R.M. Slawson, Potential repair of *Escherichia coli* DNA following exposure to UV radiation from both medium- and low-pressure UV sources used in drinking water treatment, Appl. Environ. Microbiol. 68 (2002) 3293-3299. https://doi.org/10.1128/AEM.68.7.3293-3299.2002.

[60] J.L. Zimmer-Thomas, R.M. Slawson, P.M. Huck, A comparison of DNA repair and survival of *Escherichia coli* O157:H7 following exposure to both low- and medium- pressure UV irradiation, J. Water Health. 5 (2007) 407-415. https://doi.org/10.2166/wh.2007.036.

[61] B. Van Houten, Nucleotide excision repair in Escherichia coli, Microbiol. Rev. 54 (1990) 18-51.

[62] L. Lee, K. Wilson, The Reactive-Diffusive Length of OH and Ozone in Model Organic Aerosols, J Phys Chem A. 120 (2016) 6800-6812. https://doi.org/10.1021/acs.jpca.6b05285.

[63] P. Sun, C. Tyree, C.-. Huang, Inactivation of Escherichia coli, Bacteriophage MS2, and Bacillus Spores under UV/H_2O_2 and UV/Peroxydisulfate Advanced Disinfection Conditions, Environ. Sci. Technol. 50 (2016) 4448-4458. https://doi.org/10.1021/acs.est.5b06097.

[64] V. Shafirovich, A. Dourandin, W. Huang, N.E. Geacintov, The Carbonate Radical Is a Site-selective Oxidizing Agent of Guanine in Double-stranded Oligonucleotides, J. Biol. Chem. 276 (2001) 24621-24626. https://doi.org/10.1074/jbc.M101131200.

[65] M.S. Koo, X. Chen, K. Cho, T. An, W. Choi, In Situ Photoelectrochemical Chloride Activation Using a WO3 Electrode for Oxidative Treatment with Simultaneous H_2 Evolution under Visible Light, Environ. Sci. Technol. 53 (2019) 9926-9936. https://doi.org/10.1021/acs.est.9b02401.

[66] W.R.P. Barros, T. Ereno, A.C. Tavares, M.R.V. Lanza, In Situ Electrochemical Generation of Hydrogen Peroxide in Alkaline Aqueous Solution by using an Unmodified Gas Diffusion Electrode, ChemElectroChem. 2 (2015) 714-719. https://doi.org/10.1002/celc.201402426.

[67] S. Siahrostami, A. Verdaguer-Casadevall, M. Karamad, D. Deiana, P. Malacrida, B. Wickman, M. Escudero-Escribano, E.A. Paoli, R. Frydendal, T.W. Hansen, I. Chorkendorff, I.E.L. Stephens, J. Rossmeisl, Enabling direct H_2O_2 production through rational electrocatalyst design, Nat. Mater. 12 (2013) 1137. https://doi.org/10.1038/nmat3795

[68] Y. Sun, I. Sinev, W. Ju, A. Bergmann, S. Dresp, S. Kühl, C. Spöri, H. Schmies, H. Wang, D. Bernsmeier, B. Paul, R. Schmack, R. Kraehnert, B. Roldan Cuenya, P. Strasser, Efficient Electrochemical Hydrogen Peroxide Production from Molecular Oxygen on Nitrogen-Doped Mesoporous Carbon Catalysts, ACS Catal. 8 (2018) 2844-2856. https://doi.org/10.1021/acscatal.7b03464.

[69] J.O. Thomsen, F. Ngaboyamahina, K.L. Sellgren, B.T. Hawkins, J.R. Piascik, E.J.D. Klem, B. Parker, M.A. Deshusses, B.R. Stoner, J.T. Glass, Enhanced H2O2 Production at Reductive Potentials from Oxidized Boron-Doped Ultrananocrystalline Diamond Electrodes, ACS Appl. Mater. Interfaces. 9 (2017) 16610-16619. https://doi.org/10.1021/acsami.7b01614.

[70] D.A. Lytle, E.W. Rice, C.H. Johnson, K.R. Fox, Electrophoretic mobilities of Escherichia coli O157:H7 and wild-type *Escherichia coli* strains, Appl. Environ. Microbiol. 65 (1999) 3222-3225.